Over What Area Did the Oil and Gas Spread During the 2010 Deepwater Horizon Oil Spill?

By Tamay M. Özgökmen,
Eric P. Chassignet,
Clint N. Dawson,
Dmitry Dukhovskoy, Gregg Jacobs,
James Ledwell,
Oscar Garcia-Pineda,
Ian R. MacDonald, Steven L. Morey,
Maria Josefina Olascoaga,
Andrew C. Poje, Mark Reed,
and Jørgen Skancke

ABSTRACT. The 2010 Deepwater Horizon (DWH) oil spill in the Gulf of Mexico resulted in the collection of a vast amount of situ and remotely sensed data that can be used to determine the spatiotemporal extent of the oil spill and test advances in oil spill models, verifying their utility for future operational use. This article summarizes observations of hydrocarbon dispersion collected at the surface and at depth and our current understanding of the factors that affect the dispersion, as well as our improved ability to model and predict oil and gas transport. As a direct result of studying the area where oil and gas spread during the DWH oil spill, our forecasting capabilities have been greatly enhanced. State-of-the-art oil spill models now include the ability to simulate the rise of a buoyant plume of oil from sources at the seabed to the surface. A number of efforts have focused on improving our understanding of the influences of the near-surface oceanic layer and the atmospheric boundary layer on oil spill dispersion, including the effects of waves. In the future, oil spill modeling routines will likely be included in Earth system modeling environments, which will link physical models (hydrodynamic, surface wave, and atmospheric) with marine sediment and biogeochemical components.

INTRODUCTION

The 2010 Deepwater Horizon (DWH) oil spill in the Gulf of Mexico (GoM) underscored the need for an immediate and informed response at the onset of such a disaster. It is imperative to be able to quickly answer questions such as: Where will the oil go? How fast will it get there? How much oil will be transported? The answers help determine the allocation of limited response resources and ultimately the socioeconomic and environmental impacts of a spill. The benefit of predictive capability during events such as an oil spill is analogous to the forecasting of any natural disaster—it allows individuals, entire communities, and emergency planners to take necessary measures to respond. The need for this capability, particularly with regard to potential oil spills, is urgent because of the ongoing construction of deepwater rigs. We require a much better understanding of the spatially and temporally varying transport pathways

between these rigs and the coastline than we had during the DWH oil spill.

This article has two main goals: (1) to summarize the area over which the DWH oil spill spread, and (2) to highlight the progress made, since the 2010 event, in understanding the processes responsible for the spreading of released hydrocarbons and in forecasting hydrocarbon dispersion.

OBSERVATIONS OF AN OIL SPILL

Assessment of floating oil distribution and magnitude is necessary for quantifying the extent of an oil spill and providing accurate initial conditions to oil spill prediction models. Because it is not always practical to conduct extensive in situ measurements in the aftermath of a spill, assessments rely heavily on remote-sensing data analysis. Relevant remote-sensing techniques include optical, microwave, and radar sensors set up on aircraft and satellites (Leifer et al., 2012). Of these, synthetic aperture radar (SAR) has proven its ability to detect floating oil for response and assessment of oil spills over 30 years of operational use (Holt, 2004). SAR data are particularly useful during an oil spill event because oil spills (and the resulting movement of hydrocarbons) continue 24/7, without regard for day or night visibility. However, SAR imagery may be limited by certain

weather conditions (Garcia-Pineda et al., 2009). Satellite imagery in the visible and near infrared (NIR) has also been widely used to delineate oil slicks in the ocean (Hu et al., 2003). Recently, the wider availability of medium-resolution (250 m and 300 m) MODIS and MERIS data made it also possible to use these wide-swath (2,330 km and 1,150 km, respectively) satellite instruments for cost-effective spill monitoring in near-real time. Airborne remote sensing is another very useful technique, as it provides higher temporal and spatial resolution than satellite remote sensing; however, it is not as cost-effective. It provides only a partial overview of the affected areas, and it can be slow to process and distribute.

The geographic source of the DWH discharge was essentially constant during the 87 days of flow, but physical details of the release points underwent substantial changes as responders gradually regained well control. The critical shift was amputation of the fallen risers on June 2–3. Prior to this action, discharges were dispersed among several points of failure along the fallen pipes; after, the entire discharge escaped from a single point atop the dysfunctional blowout preventer. Although the gross flow rate then increased, recapture of oil and treatment with dispersants reduced the net discharge until installation of the riser stack on July 15 ended all releases (Lehr et al., 2010; McNutt et al., 2012). Therefore, the two periods, April 20 to June 1 and June 2 to July 15, offered significantly different conditions, which potentially affected the subsequent distribution and fate of the oil. Remote-sensing data provided a means for tracking a critical component of this discharge—movement of oil across the ocean surface. It is this component of the oil that generated contaminated marine snow (Passow, 2014), injured mesophotic corals (Silva et al., 2016; Etnoyer et al., 2016), and oiled over 2,100 km of the Gulf Coast (Nixon et al., 2016).

SAR imaging of surface oil commenced on April 24 and continued at high capacity

OPPOSITE. Dye release during the Surfzone Coastal Oil Pathway Experiment (SCOPE) as captured from a tethered balloon. The dye was released outside of the surf zone, but did not make land fall during the four hours of aerial observation because of processes involved in the interaction of the surf zone with the inner shelf, as well as a 2 m thick buoyant flow released from a tidal inlet. These processes influence which coastlines will be most impacted by oil spills. *Photo credit: Guillaume Novelli*

through August 3, after which floating oil was no longer detected. MacDonald et al. (2015) analyzed 166 SAR images collected during this period; they used Texture Classifying Neural Network Algorithm (TCNNA) routines (Garcia-Pineda et al., 2009) to delineate areas of water covered by thin (~1 μm) oil and Oil Emulsion Detection Algorithm (OEDA) routines (Garcia-Pineda et al., 2013) to detect much smaller areas of thick (~70 μm) oil.

Interpolation among the images produced a continuous time series of gridded values for floating oil and oil emulsion (m³ km⁻²) in 5 × 5 km cells across the impacted region (MacDonald et al., 2015). The surface oil covered a large and dynamically amorphous region that was focused over the release point but continuously driven into different distribution patterns over a 149,000 km² area of the northeastern Gulf under changing wind and current effects. Figure 1 (upper panel) shows the average values in these cells for April 24 to August 3. Analysis of the daily aggregated values shows two prominent features of the surface oil. First, the magnitude of oil was highly sensitive to wind speeds; throughout the emergency, surface oil that was visible to SAR decreased sharply when winds exceeded about 5 m s⁻¹ and then gradually increased when winds subsided (Figure 1, lower
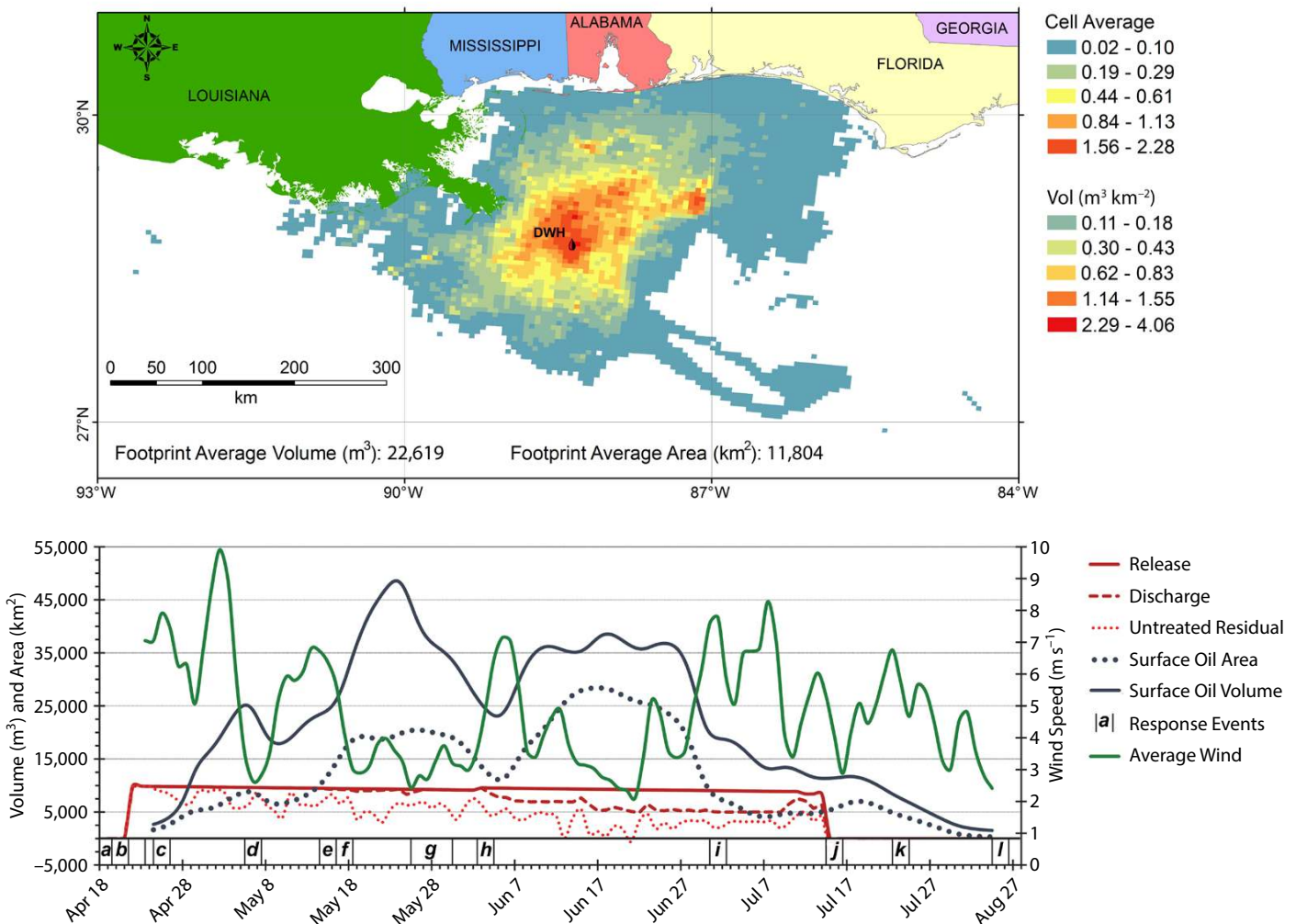

FIGURE 1. (upper panel) Distribution and average volume of surface oil (m³ km⁻²) from Deepwater Horizon (DWH) discharge, gridded at 5 × 5 km scale across a cumulative footprint of 149,000 km², April 24– August 3, 2010. Data were derived from 169 synthetic aperture radar (SAR) images acquired during this interval and processed using Texture Classifying Neural Network Algorithm (TCNNA) and Oil Emulsion Detection Algorithm (OEDA) techniques. (lower panel) Time series of DWH discharge plotted with surface oil and average wind speeds. Release magnitudes show best daily estimates of oil escaping from the damaged well. Discharge subtracts the oil recovered from the gross release, while treatment further subtracts oil burned and dispersed by aerial and subsea applications of Corexit at maximum efficacy. Response events potentially affected the spread of surface oil: (a) Macondo well blowout occurs. (b) DWH drill rig sinks and release begins. (c) Aerial dispersant application begins. (d) Containment dome attempt fails, and burning of surface oil begins. (e) Subsea dispersant campaign begins (May 5). (f) Flaring of recovered oil begins. (g) Top kill attempt. (h) The riser is cut from the blowout preventer, and direct injection of subsea dispersant begins. (i) Hurricane Alex makes landfall. (j) Capping of the stack closure stops release of oil. (k) Tropical Storm Bonnie makes landfall. (l) The well is killed by static backfill. *From MacDonald (2015) and MacDonald et al. (2015)*

panel). Second, there is a state change in the geographic concentration and distribution of surface oil when the pre- and post-riser removal periods are compared. In summary, the total detected volume of oil decreased by 21% after riser removal. However, probably due to increased treatments with Corexit (a dispersant), the ocean area over which the remaining oil was dispersed increased by 49% (Figure 1, lower panel). At face value, this result is consistent with the efficacy of response efforts to reduce surface oil by recapture and burning operations (Lehr et al., 2010) and with the subsea application of dispersant. This benefit has to be weighed against increased exposure of planktonic larvae and pelagic organisms to oil, which can produce deleterious effects to developing fish even at very low concentrations (Incardona et al., 2014).

FACTORS AFFECTING HYDROCARBON DISPERSION IN THE ENVIRONMENT

In order to model the area over which the DWH oil and gas spread, it is necessary to have a basic understanding of the factors that affect hydrocarbon dispersion in the environment. Figure 2 shows the complexity of the physical processes that govern particle transport in the aftermath of a deepwater oil or gas spill. Initially, the DWH spill was produced by the high-pressure efflux of a hot, multiphase mixture of oil and gas at several sites in the broken riser pipe. Containment efforts involved cutting the riser pipe to isolate the release to a single, nominally 0.5 m diameter, source (McNutt et al., 2011) and application of chemical dispersants in efforts to minimize the size and therefore maximize the subsurface mixing of oil droplets. A multiphase turbulent jet issuing from the source rapidly transitions to a multiphase turbulent plume that mixes with ambient fluid by entrainment processes. The buoyancy fluxes associated with the DWH spill are extremely large—the oil buoyancy anomaly alone was equivalent to a heat flux of 1 GW m^{-2} (1 GW = 10^9 W; Reddy et al., 2012), with the accompanying gases providing anomalies five times larger. Such buoyancy fluxes, two orders of magnitude larger than those of deep ocean thermal vents (Speer and Marshall, 1995), and greater still than those associated with cold air outbreaks at the ocean surface, imply that the resulting plume does not simply passively advect through the rotating, stratified water column, but is instead capable of driving local dynamic processes.

Turbulent levels at the source, along with the application of chemical dispersants, minimized the mean size of oil droplets, effectively reducing the oil slip velocity relative to seawater and increasing the droplet rise time. Given the ambient environmental stratification and the levels of turbulence generated by the extreme buoyancy fluxes associated with the spill, the resulting plume was expected to be characterized by multiple lateral intrusion levels, where downdrafts of negatively buoyant ambient fluid suppress the rise of positively buoyant oil and gas (Asaeda and Imberger, 1993; Socolofsky and Adams, 2005). Discrete subsurface maxima of constituent hydrocarbon concentrations were observed in the aftermath of the incident (Reddy et al., 2012; Spier et al., 2013).

When hydrocarbons do eventually reach the surface, they are strongly influenced by air-sea forcing, and there are several identifiable stages of transport, including (1) surface dispersion under the action of mixed layer dynamics,
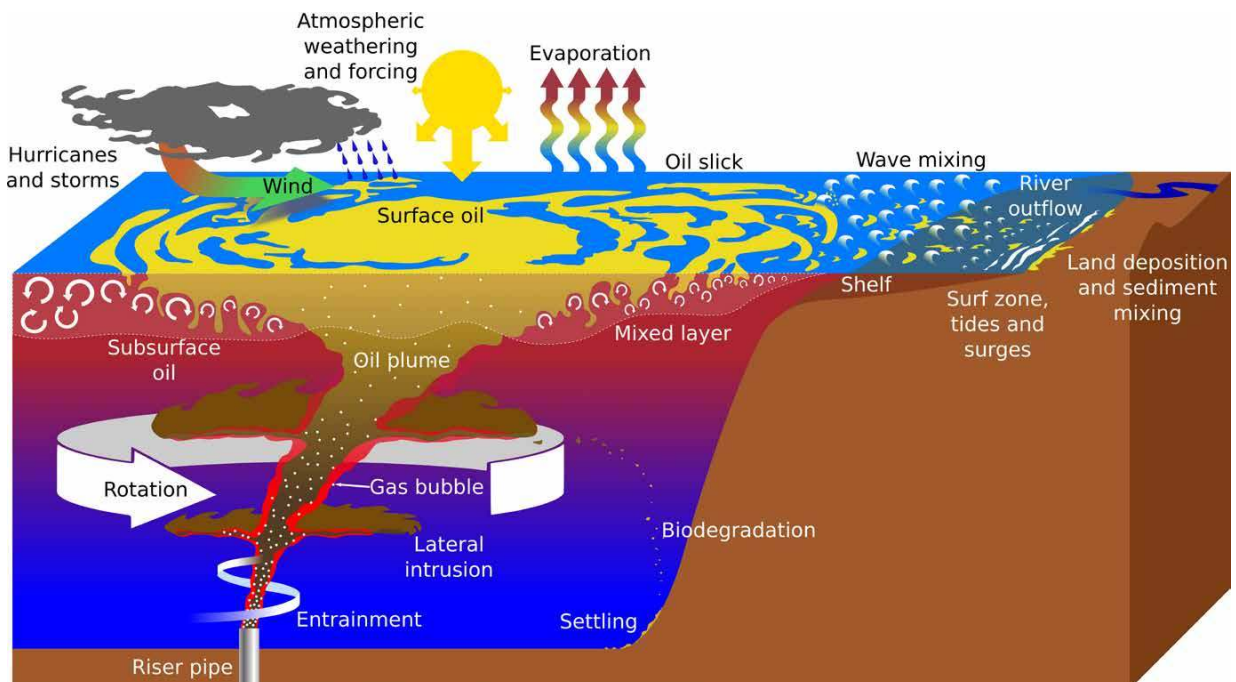

FIGURE 2. Schematic depiction of transport processes in a subsurface spill.

mesoscale currents, wind, and waves, including tropical storm conditions; (2) release of gas into the atmospheric boundary layer by air-sea interaction processes through the burning of surface oil; (3) transport of gas in the atmosphere; and (4) transport to the coast across the inner shelf and surf zone (Figure 2).

An aerial photograph taken during the DWH event (Figure 3, upper panel) shows a striking example of how the complex interactions between the atmosphere and the ocean shape the oil distribution along the boundary of these large systems. Figure 3 (lower panel) illustrates a general classification of transport processes near the ocean's surface. At scales of 1 m to 100 m, and 1 s to a few hours, fully three-dimensional turbulent processes dominate the boundary layer dynamics. At scales of 100 m to 10 km, and O(1) day,

the so-called submesoscale processes critically impact transport and mixing in the upper ocean, modify mixed-layer stratification, and dominate relative dispersion of near-surface material (Capet et al., 2008a,b; Zhong et al., 2012, Özgökmen et al., 2012a,b). Stokes drift from surface waves and Ekman transport from wind stress combine to form the near-surface current that advects oil. The depth of this current is controlled by boundary layer turbulence, including Langmuir circulations, that are driven by air-sea fluxes and surface waves. Surface convergences above the Langmuir downwelling zones concentrate oil into along-wind streaks, as do larger-scale convergences at fronts. Frontal submesoscale eddies can move oil across these fronts. The vertical velocities in the boundary layer and at the fronts mix oil into the boundary layer and below

it. These processes combine to distribute material concentrations in a very different manner than expected when considering only the mesoscale flows (10 km to 100 km, and days to months, for example, a Loop Current eddy in the Gulf of Mexico). Thus, the impacts of processes over a wide range of spatial and temporal scales on the eventual oil distribution must also be taken into account when responding to an oil spill.

EXPERIMENTAL STUDIES OF OIL AND GAS TRANSPORT PROCESSES

Since the DWH oil spill, a great deal of research has been undertaken to understand the dynamics of the processes behind the transport of hydrocarbons released in the marine environment. Here, we review some of these
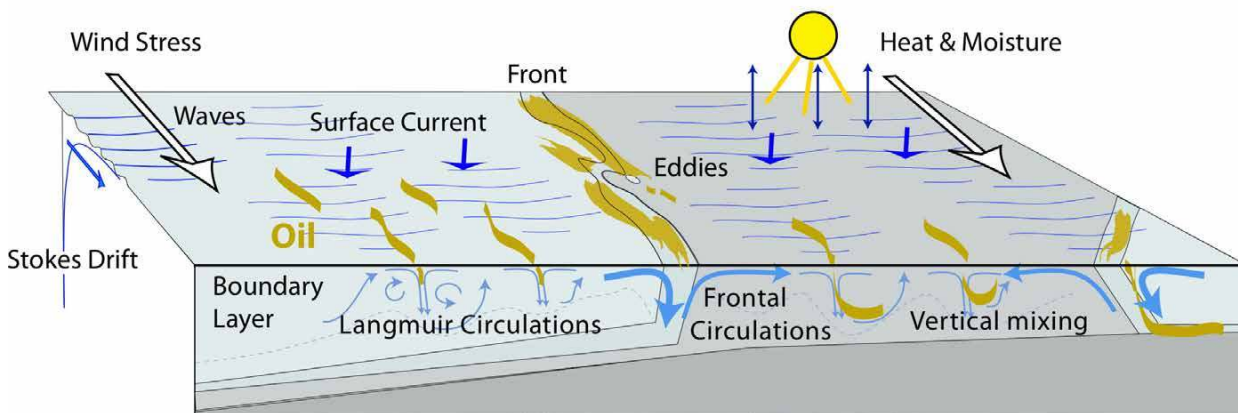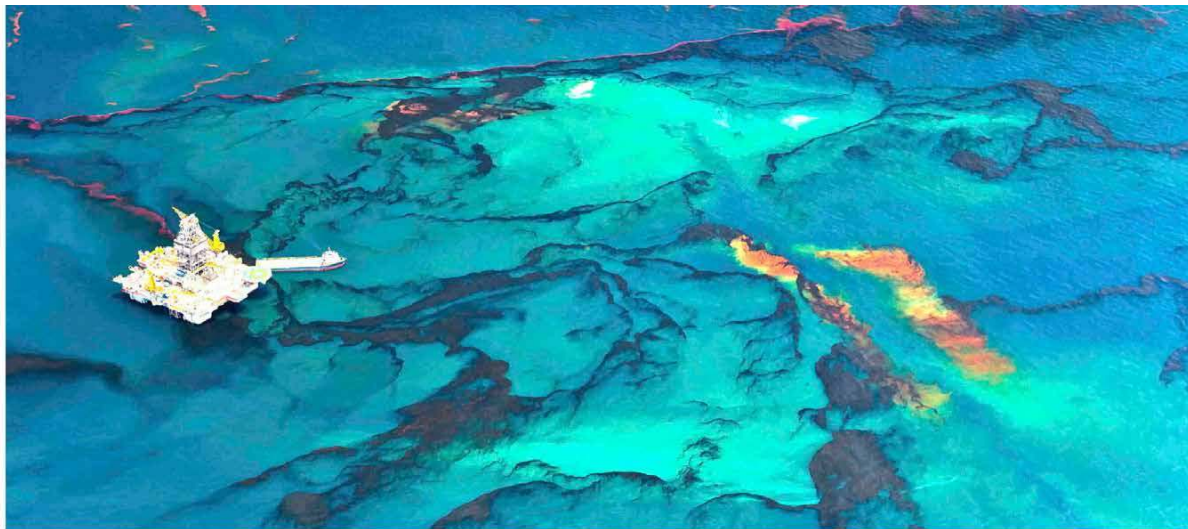

FIGURE 3. (upper panel) Aerial photo of surface oil during the Deepwater Horizon spill (reproduced through an agreement with D. Beltra). (lower panel) Illustration of surface ocean transport processes.

experimental studies of mechanisms relevant to transport of hydrocarbons at the ocean surface and at depth in the northern Gulf of Mexico.

Surface Dispersion Experiments

As discussed in the previous section, the surface extent and movement of the DWH oil spill resulted from interaction of motions at different scales. During May 2010, a few weeks into the spill, the core of the Loop Current was located about 150 km south of the oil spill site, too far to directly affect the spreading of the oil. However, mesoscale cyclonic eddies on the edge of the Loop Current did substantively affect the spreading of the oil as they controlled the development of a large finger in the oil slick, referred to as a "tiger tail," as well as the accumulation of oil on the northeastern side of the spill site during May–June 2010 (Olascoaga and Haller, 2012; Olascoaga et al., 2013). Intense southeast winds associated with Hurricane Alex, which developed in late June, eventually caused a reduction of the surface oil extent at the end of June and the beginning of July (Figure 1, lower panel), as oil was driven onshore and mixed underwater (Goni et al., 2015).

Interactions between different scales of motion, namely submesoscales and mesoscales, may have played an important role in the dispersion of the spilled oil during the DWH event, as revealed by satellite images. Observations sufficiently dense to permit extraction of material patterns on multiple scales are limited. To fill this void, the Grand LAgrangian Deployment (GLAD) experiment (Figure 4 upper panel) was conducted in the summer of 2012. GLAD was the largest synoptic surface drifter deployment in oceanography to date, with 317 Lagrangian instruments launched in clusters in DeSoto Canyon, the location of the DWH spill, over 10 days. Conditions sampled over the subsequent six months ranged from calm to extreme (Hurricane Isaac). While dynamics at submesoscales (100 m to 10 km) are well defined by recent research (Capet et al., 2008a,b; Fox-Kemper

and Ferrari, 2008; D'Asaro et al., 2011; Mensa et al., 2013), the investigation of their effects on material transport by the ocean has been mostly based on modeling (Poje et al., 2010; Haza et al., 2012; Özgökmen et al., 2012a,b) because observations are still very rare (Shcherbina et al., 2013). Also, the details of the establishment, maintenance, and energetics of such features in the GoM remain unclear. Lagrangian experiments are currently the most accurate way to quantify

the net effect of all flow scales on ocean transport. The intensive drifter deployments in the GLAD experiment revealed submesoscale dispersion during the summer in DeSoto Canyon (Poje et al., 2014) and mesoscale-dominated dispersion in the interior of the Gulf (Olascoaga et al., 2013). GLAD observations allowed quantification of the amount of scale-dependent dispersion that is missing in current operational circulation models and satellite altimeter-derived velocity
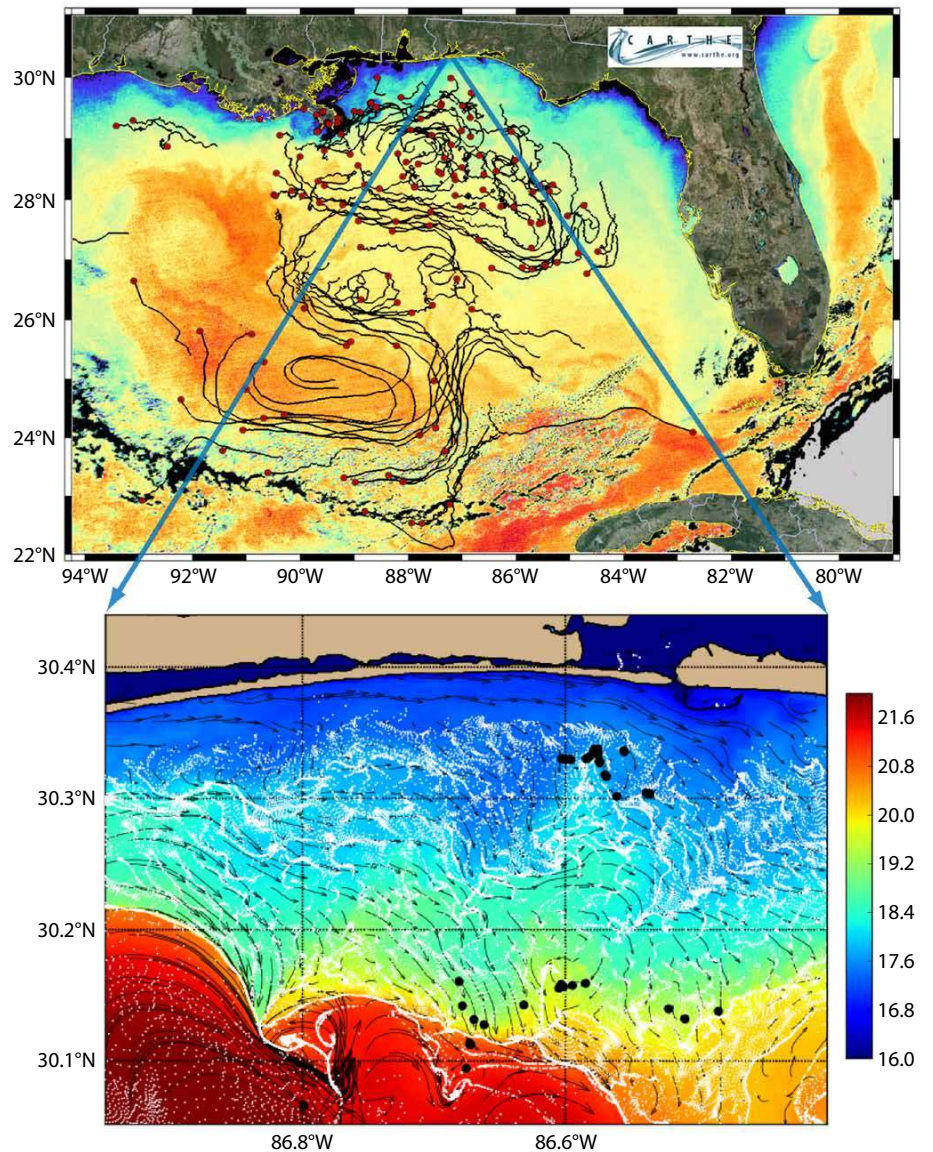
FIGURE 4. Grand LAgrangian Deployment (GLAD) drifter trajectories three months after release near the Deepwater Horizon region, superimposed on satellite sea surface temperature. Navy Coastal Ocean Model (NCOM) simulation for SCOPE, resolving frontal structures trapping and transporting surface particles (shown in white) in comparison to real drifters (black circles). Most modeled and real drifters aligned along fronts, implying a critical role for coastal fronts in trapping and transporting surface material.

fields. Subsequently, GLAD observations have been used to assess and improve predictions from models and satellite-altimeter data sets (Carrier et al., 2014; Jacobs et al., 2014; Berta et al., 2015; Coelho et al., 2015).

The Surfzone Coastal Oil Pathway Experiment (SCOPE; Figure 4 lower panel and title page photo) was conducted in December 2013 to measure the inner shelf and surf zone processes responsible for the "last mile" of oil transport. The intensive three-week campaign consisted of a cross-shore array of fixed instrumentation to measure background wind, waves, currents, and water properties from 10 m water depth to the shoreline; Lagrangian observations (180 GPS-equipped surface drifters, fluorescent dye); and moving-vessel measuring platforms (small vessels, wave runners, and unmanned subaqueous and aerial vehicles). One of the primary findings during SCOPE was that surface convergence zones, created by freshwater fronts from estuaries by tidal exchange, appear to control the distribution of surface material near the coast (Figure 4 lower panel; Hugenard et al., 2015).

Deep Dispersion Experiments

In late July 2012, a passive tracer was released near the site of the DWH eruption (Ledwell et al., 2016). Tracer dispersion was studied through August 2013 to quantify the fate of material accidentally or naturally released along the West Florida slope. The tracer, deployed near the depth of the DWH plume that was found near 1,100 m depth by Camilli et al. (2010) moved westward, following isobaths at first, and then dispersed over much of the northern Gulf (see Figure 5; Ledwell et al., 2016). Mixing of the tracer, both across and along density surfaces, was greatly enhanced by energetic flows over the ridges and salt domes of the West Florida slope. Hurricane Isaac, which passed over the site about a month after the tracer release, generated particularly strong currents along the slope. Homogenization of the tracer along isopycnal surfaces by stirring and small-scale mixing was much more rapid than in the open ocean thermocline. Nevertheless, streakiness of the tracer distribution persisted over the whole period, though it steadily declined. Peak concentrations fell to 10^{-8} of the concentration in the initial plume after 12 months. A numerical simulation of the tracer dispersion, conducted at North Carolina State University using the South Atlantic Bight and Gulf of Mexico (SABGOM) general circulation model, reproduced fairly well the statistics that are important to environmental impact, such as changes with time and spatial autocorrelation of concentrations (Ledwell et al., 2016).

MODELING AND PREDICTING OIL AND GAS TRANSPORT

Model predictions of the evolution of an oil spill in the ocean are typically performed by computing the movement of large numbers of simulated discrete "particles," each representing a volume of oil or related constituents. Oil spill models vary in dimensional complexity, simulating (1) only the movement of oil floating on the surface, a two-dimensional computation; (2) the three-dimensional movement of oil in the water column, allowing for oil to submerge and resurface; or (3) the full life cycle of hydrocarbons released from a subsurface blowout through a buoyant plume to the surface, with dissolution of some components into subsurface layers. Models also incorporate different levels of sophistication to simulate various constituents of the hydrocarbons being released and their modification through chemical alteration, emulsification, and biological activity (processes often collectively termed "weathering"), as well as response activities such as skimming, burning, and application of surfactants.

Surface Oil Drift Modeling

A decades-old methodology for modeling an oil spill is to advect simulated particles in a velocity field that is some function of the surface current and near-surface
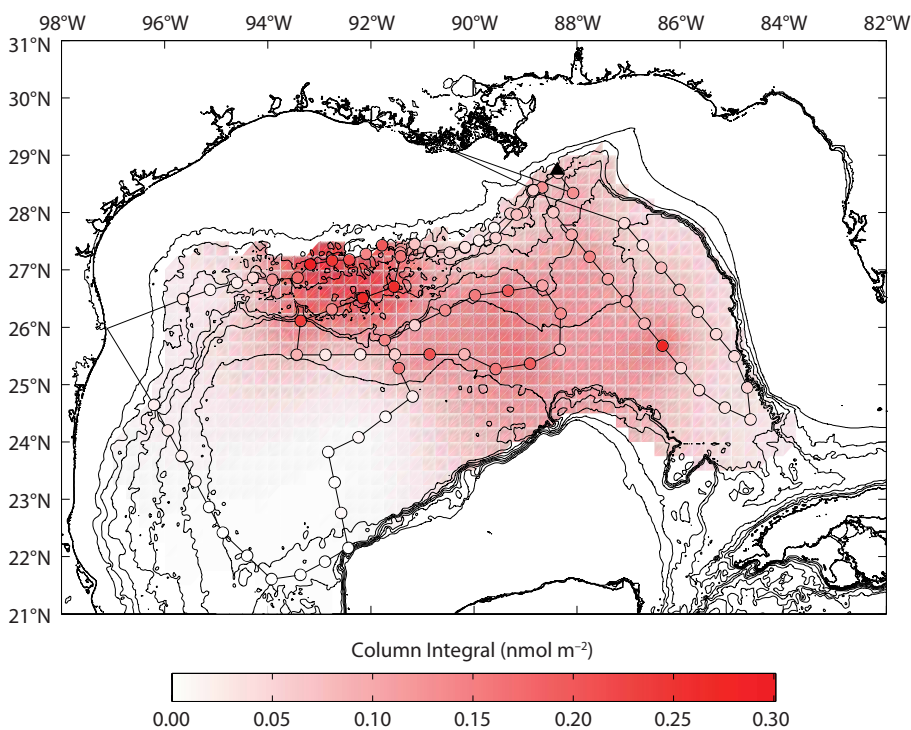

FIGURE 5. Distribution of the tracer 12 months after it was released near the site of the DWH rupture. The sampling stations are indicated by circles, colored with the column integral of tracer found. The background color is a smoothed map of tracer distribution based on these sampling stations. The isobaths are plotted every 500 m.

wind. An often used method has been to add to the ocean surface current vector an additional velocity vector that is some fraction of the wind speed (often 3.5%, the so-called "3.5% rule") in magnitude directed at some clockwise rotation from the wind direction. These methods have evolved from using a constant 20° clockwise rotation (Smith et al., 1982) to wind-speed dependent rotation angles (Samuels et al., 1982). These approaches were developed to account for processes, such as Ekman and Langmuir dynamics, that are unresolved near the surface in ocean circulation models. Comparison of forecasts from these types of oil spill models forced by mesoscale eddy-resolving ocean model currents and winds from operational weather models to drogued and oil-following drifters (Reed et al., 1988) have been disappointingly low (Price et al., 2006). Recent advances in numerical models now permit horizontal resolutions as fine as 20 m to 50 m on the coast and 1 km in the deep water. Since the DWH event, forecasting advancements can be attributed to both increased capability in numerical models and a better understanding of the processes controlling the oil dispersion, specifically those due to ocean currents and the impact of near-surface processes such as Stokes drift and Langmuir circulation (Le Hénaff et al., 2012; Curcic et al., 2016).

In addition to the basic geostrophic deepwater dynamics that played a major role in dispersing the oil during the DWH event (Walker et al., 2011; e.g., the Loop Current eddy and associated peripheral cyclones as discussed above), Ekman drift, in particular, was a significant factor (Liu et al., 2014). This was demonstrated by computing trajectories calculated from geostrophic currents determined from sea surface height maps with and without an Ekman drift added. Current trajectories were compared to drifters released during the DWH event to demonstrate improved prediction with Ekman drift. Numerical models with sufficient vertical resolution represent the Ekman

drift, and additional parameterizations of Stokes drift and Langmuir effects can further improve prediction skills (Le Hénaff et al., 2012). The importance of considering the near-surface wind-driven processes was evident from retrospective model studies of the DWH event. The generally southerly winds that occurred throughout that time period were shown to have helped prevent oil distribution beyond the GoM. Without the effects of the wind drift, simulations show that oil would likely have reached the Straits of Florida by the middle of May 2010. In addition, the wind drift altered the distribution of oil along the coastline, sparing Florida significantly greater impact from oil coming ashore. The Mississippi River outflow was also shown to have impacted the DWH oil transport (Kourafalou and Androulidakis, 2013).

Oil Spill Predictive Modeling

Oil spill models, such as the General NOAA Operational Modeling Environment (GNOME) used operationally during the DWH event, were primarily computations of surface trajectories of oil-simulating particles. Though GNOME has the ability to simulate weathering effects, it was run operationally during the DWH spill simply as a conservative particle advection model with random diffusion (MacFadyen et al., 2011). For forecasting purposes, the model was initialized with the location of the surface slick daily as determined from aircraft and satellite observations, and it was run forced by currents and winds from ocean and weather model forecasts. Multiple ocean current and wind forecast products permitted ensembles of predictions to be run. Differences in the individual ensemble members highlight the substantial uncertainty in oil spill trajectory forecasts that arises from the uncertainty in wind and ocean current forcing (MacFadyen et al., 2011, their Figure 5).

Operational oil spill forecasts during the DWH spill were performed on short (72-hour) time horizons using particle trajectory models that did not include

detailed oil weathering effects. However, these effects are crucial to the accuracy of long-term predictions of the total area to be affected by an oil spill or the amount of oil arriving on shorelines. As an example, a computation performed by the National Center for Atmospheric Research simulated the movement of a passive tracer released from the DWH site over several months in order to provide an estimate of the envelope for possible oil dispersal scenarios. The simulation showed oil exiting the GoM and flowing northward along the Atlantic coast with the Gulf Stream and eastward through the Atlantic becoming progressively diluted with distance (Klemas, 2010). No indication of the presence of hydrocarbons from the DWH has been found this far from the source in the Atlantic, though; we note that these model scenarios did not include weathering effects leading to the dissipation of oil. In contrast, a series of simulations run with a simple oil spill particle advection model that accounts for weathering of oil, parameterized by random removal of oil particles based on a prescribed half-life, was in good agreement with SAR-derived maps of oil coverage during the DWH time period (Figure 1). Objective comparisons between simulated time-composited oil coverage and that derived from SAR data show that the simulated coverage of oil best agrees with the SAR-observed oil coverage when oil is removed from the model with a half-life between three and six days (Morey et al., 2011; Dukhovskoy et al., 2015).

One of the consistent points revealed and reinforced by the research is that scarcity of observations is a critical factor limiting predictive skill (Mariano et al., 2011). Satellite altimeters typically provide only one to two ground tracks daily, and even using the three satellites available during DWH, forecast skill was strongly affected. Work supported by the Gulf of Mexico Research Initiative (GoMRI) brought a range of targeted observational capabilities to the GoM. Perhaps one of the most promising was drifter observations,

which can be employed at low cost and persist in an area of interest. Results of assimilating the GLAD drifter observations indicate significant advancement in drift trajectory forecasting (Carrier et al., 2014; Muscarella et al., 2015). Evaluation of the impact of specific observations can be performed using Observation System Simulation Experiments (OSSE), which has long been a basis for building support for meteorological instruments. Correctly configuring OSSE is challenging, yet there are recent examples of ocean applications (Halliwell et al., 2015). Even as observations are added and models advance, it is important to remember that errors will persist at some level. The methods for forecasting state errors for the ocean are typically through ensembles. Wei et al. (2014) showed that the small errors in ocean state, which imply small errors in the positions of ocean eddy features, lead to large uncertainties in the forecast drift trajectory.

The problem of forecasting particle trajectories is much more challenging than that posed in traditional ocean prediction, where the primary focus has been on predicting mesoscale velocity and density fields. Recent advancements in modeling particle trajectories have been made by correcting the background flow field with observed trajectories. Coelho et al. (2015) demonstrated an ensemble approach that combines the forecasts from different forecast systems, weighted to provide an optimal forecast, while Berta et al. (2015) used a background geostrophic velocity field from sea surface height and observed velocities to construct an optimal forecast trajectory. Such approaches offer advantages over traditional data assimilation systems, as dynamical balances between variables are not required. Advancement from the predictive capability prior to the DWH event can be illustrated by comparing the work of Price et al. (2006) to more recent studies. Price et al. (2006) found position errors between ocean-following drifters and predictions to be 78 km RMS after three days. Berta et al.

(2015) and Yaremchuk et al. (2013), using more recent model configurations with the more extensive observations collected since 2010, have shown error levels are about 45 km RMS after three days. The addition of drifter trajectories to correct the background currents for the forecasts further reduced the error levels by half.

Deep-Sea Plume Modeling

Deepwater blowout plumes, such as those produced following the DWH accident, are characterized by extreme buoyancy fluxes produced by an evolving multiphase mixture of oil and gas at temperatures far above that of the ambient seawater. The resulting plumes are not passively mixed with the environmental fluid, but instead dynamically alter the local flow field. While of primary importance for remediation and response efforts, accurate prediction of how much and where the effluent will reach the surface, and the observed distribution of pollutant constituents within the water column (Reddy et al., 2012; Spier et al., 2013), poses a unique modeling challenge due to a broad range of physical and chemical processes occurring on disparate spatial and temporal scales. Modeling responses to the DWH incident have advanced along two interconnected lines. Predictive spill models, allowing detailed parameterization of droplet and bubble size distributions as well as thermochemistry, are typically based on Eulerian integral formulations of the near-field hydrodynamics and Lagrangian evolution of gas bubbles and oil droplets in the flow above the intrusion level (Adcroft et al., 2010; Yapa et al., 2012). Results from an industry-sponsored intercomparison of such models, which also allow for the parameterized effects of dispersant application at the source, are detailed in Socolofsky et al. (2015). In addition, the unique characteristics of the DWH incident have prompted research into fundamental aspects of the hydrodynamics of multiphase plumes in stratified, rotating

environments. While classical integral model predictions of primary trapping heights are in general agreement with observations of hydrocarbon concentration maxima in the vertical (Socolofsky et al., 2011), questions persist about the existence of secondary intrusion layers and observations of concentration maxima at heights much closer to the spill site. In order to begin to address these questions, detailed turbulence-resolving simulations of mixed buoyancy source, multiphase plumes using both Eulerian-Eulerian (Fabregat et al., 2015) and Eulerian-Lagrangian formulations (Fraga et al., 2016) have been conducted. Differential turbulent mixing of mixed buoyancy sources is capable of both significantly reducing the vertical extent of thermal buoyancy and producing turbulence-driven secondary intrusions of fine oil droplets above the main intrusion level, even in the complete absence of any relative velocity between oil and water phases (Fabregat Tomàs et al., in press). More dramatically, turbulence-resolving multiphase plume simulations have revealed the strong effect of system rotation on overall mixing and entrainment intrusion heights. As Figure 6 shows, Earth's rotation induces global, anticyclonic precession of the plume, greatly increasing the turbulence in the intrusion layer, leading to a significant reduction in the overall height of the plume and a significant increase in the thickness of any intrusion layers (Fabregat Tomàs et al., in press).

DISCUSSION

From analysis of observational data and modeling exercises during and following the DWH oil spill, it is clear that uncertainties in hydrodynamic/atmospheric forcing, model initialization, parameterization of unresolved processes, and weathering processes are key areas that need more study in order to improve the ability to predict the fate of an oil spill. Indeed, quantification of the uncertainty of oil spill model simulations arising from the different factors has been a

particularly active area of research since the DWH event (Gonçalves et al., 2016). Fundamentally, improvements in ocean and atmospheric model prediction will have profound impacts on the ability to forecast oil spills, even with no improvements to the most advanced oil spill models themselves. However, significant efforts have been undertaken by the oil spill research community to implement advances in the physical, chemical, and even biological dynamics of models to improve forecasting ability. State-of-the-art oil spill models now include the ability to simulate the rise of oil through a buoyant plume from sources at the seabed to the surface. As accuracy in forecasting the three-dimensional ocean velocity field improves, simulating the surfacing of oil in this manner can address the uncertainty associated with initialization of the distribution of surface oil. Consideration of the three-dimensional movement of oil also permits prediction of the spreading of oil through subsurface plumes, which was suggested by limited in situ sampling and model particle advection simulations to have occurred during the DWH spill (Camilli et al., 2010; Weisberg et al., 2011).

Downscaling from the ocean model upper-layer velocity, which may represent the average velocity over a layer several meters thick, to the true surface velocity that moves floating oil, has traditionally been parameterized using simple methods of adjusting the upper-layer currents for local winds. A number of efforts have focused on improving our understanding of the near-surface oceanic layer and atmospheric boundary layer, including the influence of waves (Le Hénaff et al., 2012; Clark et al., 2016) and the modification of wind-forced motions by the influence of floating oil on ocean surface roughness and temperature (Zheng et al., 2013).

Perhaps the most advanced recent improvement in oil spill modeling is that we have a better understanding of the size of droplets formed in the turbulent plume above the wellhead. During the spill itself, no model was able to predict the droplet size distribution, which dictates rise times, dissolution, and biodegradation, and therefore the ultimate fate of the oil. Following the spill, experimental work with down-scaled blowouts in laboratory settings led to a greatly improved model for droplet size formation (Johansen et al., 2013; Brandvik et al., 2013), which has subsequently been adopted in most state-of-the-art oil spill models (Socolofsky et al., 2015). There is good reason to believe that the impact of the DWH spill will continue to make its mark on oil spill model development in the years to come. One legacy of the DWH oil spill has been the collection of a vast amount of data, both in situ and remotely sensed, that can now be used to test advances in oil spill models and verify their utility for future operational use (https://data.gulfresearchinitiative.org).

Future enhancements will likely be inclusion of oil spill modeling routines in Earth system modeling environments, which will link physical models (hydrodynamic, surface wave, and atmospheric) with marine sediment and biogeochemical components. This coupled Earth system modeling framework will be used to simulate the interaction of oil with its environment through sedimentation and biodegradation processes. Though advances are being made in this direction, transitioning the research into demonstrated improvements for operational forecasting use will require the commitment of institutions funding basic research in oil spill modeling. 🌀
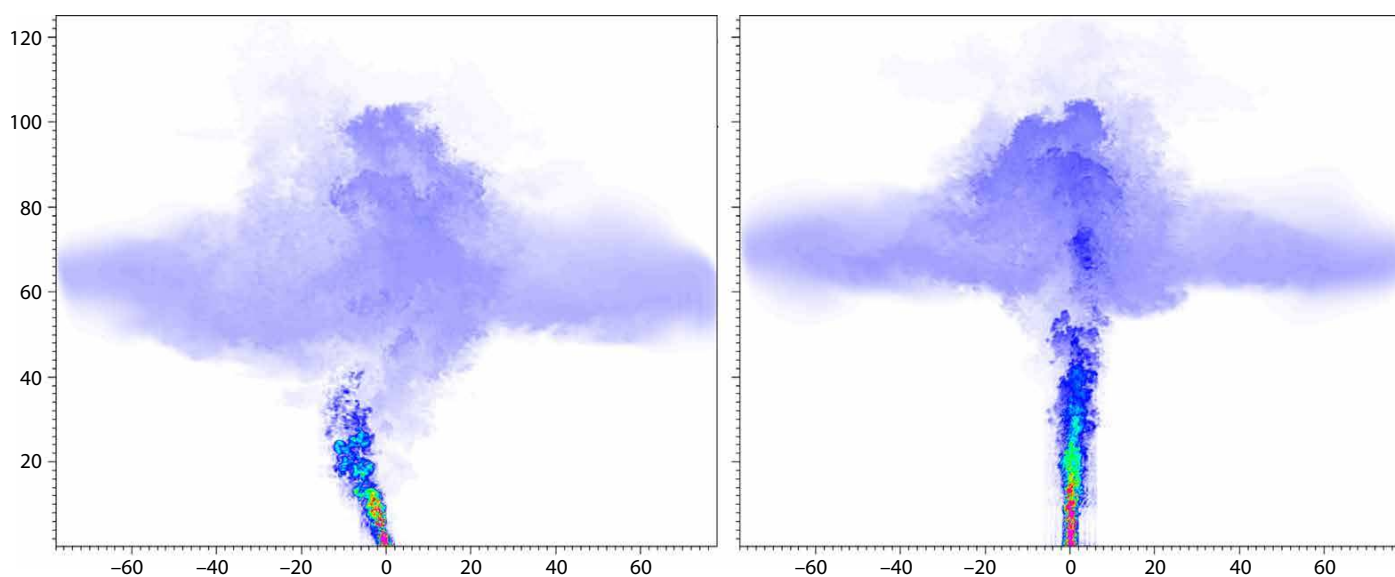

FIGURE 6. Effects of system rotation on the instantaneous oil volume fraction for a subsurface multiphase (thermal, oil, gas bubbles) blowout plume at inlet buoyancy flux and (linear) stratification approximating those of the Deepwater Horizon accident (Fabregat Tomàs et al., in press). (left panel) With ambient rotation. (right panel) Without rotation. Note the deviation from the vertical with rotation. Horizontal and vertical axes are in meters.

REFERENCES

Adcroft, A., R. Hallberg, J.P. Dunne, B.L. Samuels, J.A. Galt, C.H. Barker, and D. Payton. 2010. Simulations of underwater plumes of dissolved oil in the Gulf of Mexico. *Geophysical Research Letters* 37, L18605, http://dx.doi.org/10.1029/2010GL044689.

Asaeda, T., and J. Imberger. 1993. Structure of bubble plumes in linearly stratified environments. *Journal of Fluid Mechanics* 249:35–57.

Berta, M., A. Griffa, M.G. Magaldi, T.M. Özgökmen, A.C. Poje, A.C. Haza, and M.J. Olascoaga. 2015. Improved surface velocity and trajectory estimates in the Gulf of Mexico from blended satellite altimetry and drifter data. *Journal of Atmospheric and Oceanic Technology* 32(10):1,880–1,901, http://dx.doi.org/10.1175/JTECH-D-14-00226.1.

Brandvik, P.J., Ø.J. Johansen, F. Leirvik, U. Farooq, and P.S. Daling. 2013. Droplet breakup in subsurface oil releases: Part 1. Experimental study of droplet breakup and effectiveness of dispersant injection. *Marine Pollution Bulletin* 73(1):319–326, http://dx.doi.org/10.1016/j.marpolbul.2013.05.020.

Camilli, R., C.M. Reddy, D.R. Yoerger, B.A.S. Van Mooy, M.V. Jakuba, J.C. Kinsey, C.P. McIntyre, S.P. Sylva, and J.V. Maloney. 2010. Tracking hydrocarbon plume transport and biodegradation at Deepwater Horizon. *Science* 330:201–204, http://dx.doi.org/10.1126/science.1195223.

Capet, X., J.C. McWilliams, M.J. Molemaker, and A. Shchepetkin. 2008a. Mesoscale to submesoscale transition in the California Current system: Part I. Flow structure, eddy flux, and observational tests. *Journal of Physical Oceanography* 38:29–43, http://dx.doi.org/10.1175/2007JPO3671.1.

Capet, X., J.C. McWilliams, M.J. Molemaker, and A.F. Shchepetkin. 2008b. Mesoscale to submesoscale transition in the California Current system: Part II. Frontal processes. *Journal of Physical Oceanography* 38(1):44–64, http://dx.doi.org/10.1175/2007JPO3672.1.

Carrier, M.J., H. Ngodock, S. Smith, G. Jacobs, P. Muscarella, T. Özgökmen, B. Haus, and B. Lipphardt. 2014. Impact of assimilating ocean velocity observations inferred from Lagrangian drifter data using the NCOM-4DVAR. *Monthly Weather Review* 142(4):1,509–1,524, http://dx.doi.org/10.1175/MWR-D-13-00236.1.

Coelho, E.F., P. Hogan, G. Jacobs, P. Thoppil, H.S. Huntley, B.K. Haus, B.L. Lipphardt, A.D. Kirwan, E.H. Ryan, J. Olascoaga, and others. 2015. Ocean current estimation using a multi-model ensemble Kalman filter during the Grand Lagrangian Deployment experiment (GLAD). *Ocean Modelling* 87:86–106, http://dx.doi.org/10.1016/j.ocemod.2014.11.001.

Curcic, M., S.S. Chen, and T.M. Özgökmen. 2016. Hurricane-induced ocean surface transport and dispersion in the Gulf of Mexico. *Geophysical Research Letters* 43:2,773–2,781, http://dx.doi.org/10.1002/2015GL067619.

D'Asaro, E., C. Lee, L. Rainville, R. Harcourt, and L. Thomas. 2011. Enhanced turbulence and dissipation at ocean fronts. *Science* 332:318–322, http://dx.doi.org/10.1126/science.1201515.

Dukhovskoy, D., O. Garcia, I. MacDonald, S. Morey, and J. Ubnoske. 2015. The topological approach for objective evaluation of surface oil drift simulation. Paper presented at the 2015 Gulf of Mexico Oil Spill and Ecosystem Science Conference, Houston, TX, February 2015.

Etnoyer, P., L.N. Wickes, M. Silva, J.D. Dubick, L. Balthis, E. Salgado, and I.R. MacDonald. 2016. Decline in condition of gorgonian octocorals on mesophotic reefs in the northern Gulf of Mexico: Before and after the Deepwater Horizon oil spill. *Coral Reefs* 35:77–90, http://dx.doi.org/10.1007/s00338-015-1363-2.

Fabregat, A., W.K. Dewar, T.M. Özgökmen, A.C. Poje, and N. Wienders. 2015. Numerical simulations of turbulent thermal, bubble and hybrid plumes. *Ocean Modelling* 90:16–28, http://dx.doi.org/10.1016/j.ocemod.2015.03.007.

Fabregat Tomàs, A., A.C. Poje, T.M. Özgökmen, and W.K. Dewar. In press. Effects of rotation on turbulent buoyant plumes in stratified environments. *Journal of Geophysical Research*, http://dx.doi.org/10.1002/2016JC011737.

Fox-Kemper, B., and R. Ferrari. 2008. Parameterization of mixed-layer eddies: Part I. Theory and diagnosis. *Journal of Physical Oceanography* 38:1,145–1,165, http://dx.doi.org/10.1175/2007JPO3792.1.

Fraga, B., T. Stoesser, C.C.K. Lai, and S.A. Socolofsky. 2016. An LES-based Eulerian-Lagrangrian approach to predict the dynamics of bubble plumes. *Ocean Modelling* 97:27–36, http://dx.doi.org/10.1016/j.ocemod.2015.11.005.

Garcia-Pineda, O., I.R. MacDonald, X. Li, C.R. Jackson, and W.G. Pichel. 2013. Oil spill mapping and measurement in the Gulf of Mexico with Textural Classifier Neural Network Algorithm (TCNNA). *IEEE Journal of Selected Topics in Applied Earth Observations and Remote Sensing* 6(6):2,517–2,525, http://dx.doi.org/10.1109/JSTARS.2013.2244061.

Garcia-Pineda, O., B. Zimmer, M. Howard, W. Pichel, X. Li, and I.R. MacDonald. 2009. Using SAR images to delineate ocean oil slicks with a Texture-Classifying Neural Network Algorithm (TCNNA). *Canadian Journal of Remote Sensing* 35(5):411–421, http://dx.doi.org/10.5589/m09-035.

Goni, G.J., J.A. Trinanes, A. MacFadyen, D. Streett, M.J. Olascoaga, M.L. Imhoff, F. Muller-Karger, and M.A. Roffer. 2015. Variability of the deepwater horizon surface oil spill extent and its relationship to varying ocean currents and extreme weather conditions. Pp. 1–22 in *Mathematical Modelling and Numerical Simulation of Oil Pollution Problems*. M. Ehrhardt, ed., Springer International Publishing Switzerland, http://dx.doi.org/10.1007/978-3-319-16459-5_1.

Gonçalves, R.C., M. Iskandarani, A. Srinivasan, W.C. Thacker, E.P. Chassignet, and O.M. Knio. 2016. A framework to quantify uncertainty in simulations of oil transport in the ocean. *Journal of Geophysical Research* 121:2,058–2,077, http://dx.doi.org/10.1002/2015JC011311.

Halliwell, G.R., V. Kourafalou, M. Le Hénaff, L.K. Shay, and R. Atlas. 2015. OSSE impact analysis of airborne ocean surveys for improving upper-ocean dynamical and thermodynamical forecasts in the Gulf of Mexico. *Progress in Oceanography* 130:32–46, http://dx.doi.org/10.1016/j.pocean.2014.09.004.

Haza, A.C., T.M. Özgökmen, A. Griffa, Z.D. Garraffo, and L. Piterbarg. 2012. Parameterization of particle transport at submesoscales in the Gulf Stream region using Lagrangian subgrid-scale models. *Ocean Modelling* 42:31–49, http://dx.doi.org/10.1016/j.ocemod.2011.11.005.

Holt, B. 2004. SAR Imaging of the ocean surface. Pp. 25–80 in *Synthetic Aperture Radar Marine User's Manual*. C. Jackson and J. Apel, eds, US Department of Commerce, NOAA/NESDIS, http://www.sarusersmanual.com/ManualPDF/NOAASARManual_CH02_pg025-080.pdf.

Hu, C., F. Muller-Karger, C. Taylor, D. Myhre, B. Murch, A.L. Odriozola, and G. Godoy. 2003. MODIS detects oil spills in Lake Maracaibo, Venezuela. *Eos Transactions, American Geophysical Union* 84(33):313–319, http://dx.doi.org/10.1029/2003EO330002.

Huguenard, K.D., D.J. Bogucki, D.G. Ortiz-Suslow, N.J.M. Laxague, J.H. MacMahan, T.M. Özgökmen, B.K. Haus, A.J.H.M. Reniers, J. Hargrove, A.V. Soloviev, and H. Graber. 2016. On the nature of the frontal zone of the Choctawhatchee Bay plume in the Gulf of Mexico. *Journal of Geophysical Research* 121:1,322–1,345, http://dx.doi.org/10.1002/2015JC010988.

Incardona, J.P., L.D. Gardner, T.L. Linbo, T.L. Brown, A.J. Esbaugh, E.M. Mager, J.D. Stieglitz, B.L. French, J.S. Labenia, C.A. Laetz, and others 2014. Deepwater Horizon crude oil impacts the developing hearts of large predatory pelagic fish. *Proceedings of the National Academy of Sciences of the United States of America* 111:E1510–E1518, http://dx.doi.org/10.1073/pnas.1320950111.

Jacobs, G.A., B.P. Bartels, D.J. Bogucki, F.J. Beron-Vera, S.S. Chen, E.F. Coelho, M. Curcic, A. Griffa, M. Gough, and B.K. Haus. 2014. Data assimilation considerations for improved ocean predictability during the Gulf of Mexico Grand Lagrangian Deployment (GLAD). *Ocean Modelling* 83:98–117, http://dx.doi.org/10.1016/j.ocemod.2014.09.003.

Johansen, Ø., P.J. Brandvik, and U. Farooq. 2013. Droplet breakup in subsea oil releases: Part 2. Predictions of droplet size distributions with and without injection of chemical dispersants. *Marine Pollution Bulletin* 73(1):327–335, http://dx.doi.org/10.1016/j.marpolbul.2013.04.012.

Klemas, V. 2010. Tracking oil slicks and predicting their trajectories using remote sensors and models: Case studies of the Sea Princess and Deepwater Horizon oil spills. *Journal of Coastal Research* 26(5):789–797, http://dx.doi.org/10.2112/10A-00012.1.

Kourafalou, V.H., and Y.S. Androulidakis. 2013. Influence of Mississippi River induced circulation on the Deepwater Horizon oil spill transport. *Journal of Geophysical Research* 118(8):3,823–3,842, http://dx.doi.org/10.1002/jgrc.20272.

Ledwell, J.R., R. He, Z. Xue, S.F. DiMarco, L. Spencer, and P. Chapman. 2016. Dispersion of a tracer in the deep Gulf of Mexico. *Journal of Geophysical Research* 121:1,110–1,132, http://dx.doi.org/10.1002/2015JC011405.

Le Hénaff, M., V.H. Kourafalou, C.B. Paris, J. Helgers, Z.M. Aman, P.J. Hogan, and A. Srinivasan. 2012. Surface evolution of the Deepwater Horizon oil spill patch: Combined effects of circulation and wind-induced drift. *Environmental Science & Technology* 46(13):7,267–7,273, http://dx.doi.org/10.1021/es301570w.

Lehr, W., S. Bristol, and A. Possolo. 2010. *Oil Budget Calculator Deepwater Horizon Technical Documentation*. The Federal Interagency Solutions Group, http://www.restorethegulf.gov/sites/default/files/documents/pdf/OilBudgetCalc_Full_HQ-Print_111110.pdf.

Leifer, I., W.J. Lehr, D. Simecek-Beatty, E. Bradley, R. Clark, P. Dennison, Y. Hu, S. Matheson, C.E. Jones, B. Holt, and others. 2012. State of the art satellite and airborne marine oil spill remote sensing: Application to the BP Deepwater Horizon oil spill. *Remote Sensing of Environment* 124:185–209, http://dx.doi.org/10.1016/j.rse.2012.03.024.

Liu, Y., R.H. Weisberg, S. Vignudelli, and G.T. Mitchum. 2014. Evaluation of altimetry-derived surface current products using Lagrangian drifter trajectories in the eastern Gulf of Mexico. *Journal of Geophysical Research* 119(5):2,827–2,842, http://dx.doi.org/10.1002/2013JC009710.

Macdonald, I. 2015. Neural network analysis determination of oil slick distribution and thickness from satellite Synthetic Aperture Radar, April 24–August 3, 2010. Gulf of Mexico Research Initiative, http://dx.doi.org/10.7266/N7KW5CZN.

MacDonald, I.R., O. Garcia-Pineda, A. Beet, S. Daneshgar Asl, S., L. Feng, G. Graettinger, D. French-McCay, J. Holmes, C. Hu, I. Leifer, and others. 2015. Natural and unnatural oil slicks in the Gulf of Mexico. *Journal of Geophysical Research* 120:8,364–8,380, http://dx.doi.org/10.1002/2015JC011062.

MacFadyen, A., G.Y. Watabayashi, C.H. Barker, and C.J. Beegle-Krause. 2011. Tactical modeling of surface oil transport during the Deepwater Horizon spill response. Pp.167–178 in *Monitoring and Modeling the Deepwater Horizon Oil Spill: A Record-Breaking Enterprise*. Y. Liu, A. MacFadyen, Z.-G. Ji, and R.H. Weisberg, eds, American Geophysical Union, Washington, DC, http://dx.doi.org/10.1029/2011GM001128.

Mariano, A., V. Kourafalou, A. Srinivasan, H. Kang, G. Halliwell, E. Ryan, and M. Roffer. 2011. On the modeling of the 2010 Gulf of Mexico oil spill. *Dynamics of Atmospheres and Oceans* 52(1):322–340, http://dx.doi.org/10.1016/j.dynatmoce.2011.06.001.

McNutt, M.K., S. Chu, J. Lubchenco, T. Hunter, G. Dreyfus, S.A. Murawski, and D.M Kennedy. 2012. Applications of science and engineering to quantify and control the Deepwater Horizon oil spill. *Proceedings of the National Academy of Sciences of the United States of America* 109:20,222–20,228, http://dx.doi.org/10.1073/pnas.1214389109.

Mensa, J., A. Griffa, Z. Garraffo, T.M. Özgökmen, A.C. Haza, and M. Veneziani. 2013. Seasonality of the submesoscale dynamics in the Gulf Stream region. *Ocean Dynamics* 63:923–941, http://dx.doi.org/10.1007/s10236-013-0633-1.

Morey, S.L., D.S. Dukhovskoy, E.P. Chassignet, O. Garcia, and I. MacDonald. 2011. Objective evaluation of oil spill models using SAR imagery. Paper presented at the ASLO 2011 Aquatic Sciences Meeting, San Juan, Puerto Rico.

Muscarella, P., M.J. Carrier, H. Ngodock, S. Smith, B. Lipphardt Jr., A. Kirwan Jr., and H.S. Huntley. 2015. Do assimilated drifter velocities improve Lagrangian predictability in an operational ocean model? *Monthly Weather Review* 143(5):1,822–1,832, http://dx.doi.org/10.1175/MWR-D-14-00164.1.

Nixon, Z., S. Zengel, M. Baker, M. Steinhoff, G. Fricano, S. Rouhani, and J. Michel. 2016. Shoreline oiling from the Deepwater Horizon oil spill. *Marine Pollution Bulletin* 107:170–178, http://dx.doi.org/10.1016/j.marpolbul.2016.04.003.

Olascoaga M.J., and G. Haller. 2012. Forecasting sudden changes in environmental pollution patterns. *Proceedings of the National Academy of Sciences of the United States of America* 109(13):4,738–4,743, http://dx.doi.org/10.1073/pnas.1118574109.

Olascoaga, M.J., F.J. Beron-Vera, G. Haller, J. Trinanes, M. Iskandarani, E.F. Coelho, B. Haus, H.S. Huntley, G. Jacobs Jr., A.D. Kirwan, Jr., and others. 2013. Drifter motion in the Gulf of Mexico constrained by altimetric Lagrangian coherent structures. *Geophysical Research Letters* 40(23):6,171–6,175, http://dx.doi.org/10.1002/2013GL058624.

Özgökmen, T.M., and P.F. Fischer. 2012a. CFD application to oceanic mixed layer sampling with Lagrangian platforms. *International Journal of Computational Fluid Dynamics* 26:337–348, http://dx.doi.org/10.1080/10618562.2012.668888.

Özgökmen, T.M., A.C. Poje, P.F. Fischer, H. Childs, H. Krishnan, C. Garth, A. Haza, and E. Ryan. 2012b. On multi-scale dispersion under the influence of surface mixed layer instabilities and deep flows. *Ocean Modelling* 56:16–30, http://dx.doi.org/10.1016/j.ocemod.2012.07.004.

Passow, U. 2014. Formation of rapidly-sinking, oil-associated marine snow. *Deep Sea Research Part II* 129:232–240, http://dx.doi.org/10.1016/j.dsr2.2014.10.001.

Poje, A.C., A.C. Haza, T.M. Özgökmen, M. Magaldi, and Z.D. Garraffo. 2010. Resolution dependent relative dispersion statistics in a hierarchy of ocean models. *Ocean Modelling* 31:36–50, http://dx.doi.org/10.1016/j.ocemod.2009.09.002.

Poje, A.C., T.M. Özgökmen, B.L. Lipphart Jr., B. Haus, E.H. Ryan, A.C. Haza, G. Jacobs, A.J.H.M. Reniers, J. Olascoaga, G. Novelli, and others. 2014. Submesoscale dispersion in the vicinity of the Deepwater Horizon spill. *Proceedings of the National Academy of Sciences of the United States of America* 111(35):12,693–12,698, http://dx.doi.org/10.1073/pnas.1402452111.

Price, J.M., M. Reed, M.K. Howard, W.R. Johnson, Z.-G. Ji, C.F. Marshall, N.L. Guinasso, and G.B. Rainey. 2006. Preliminary assessment of an oil-spill trajectory model using satellite-tracked, oil-spill-simulating drifters. *Environmental Modelling & Software* 21(2):258–270, http://dx.doi.org/10.1016/j.envsoft.2004.04.025.

Reddy, C.M., J.S. Arey, J.S. Seewald, S.P. Sylva, K.L. Lemkau, R.K. Nelson, C.A. Carmichael, C.P. McIntyre, J. Fenwick, G.T. Ventura, and others. 2012. Composition and fate of gas and oil released to the water column during the Deepwater Horizon oil spill. *Proceedings of the National Academy of Sciences of the United States of America* 109(50):20,229–20,234, http://dx.doi.org/10.1073/pnas.1101242108.

Reed, M., C. Turner, M. Spaulding, K. Jayko, and D. Dorson. 1988. *Evaluation of Satellite-Tracked Surface Drifting Buoys for Simulating the Movement of Spilled Oil in the Marine Environment. Volume 2. Final Report.* Applied Science Associates, Inc., Narragansett, RI.

Samuels, W.B., N.E. Huang, and D.E. Amsiuiz. 1982. An oil spill trajectory analysis model with a variable wind deflection angle. *Ocean Engineering* 9(4):347–360, http://dx.doi.org/10.1016/0029-8018(82)90028-2.

Shcherbina, A.Y., E.A. D'Asaro, C.M. Lee, J.M. Klymak, M.J. Molemaker, and J.C. McWilliams. 2013. Statistics of vertical vorticity, divergence, and strain in a developed submesoscale turbulence field. *Geophysical Research Letters* 40:4,706–4,711, http://dx.doi.org/10.1002/grl.50919.

Silva, M., P.J. Etnoyer, and I.R. MacDonald. 2016. Coral injuries observed at mesophotic reefs after the Deepwater Horizon oil discharge. *Deep Sea Research Part II* 129:96–107, http://dx.doi.org/10.1016/j.dsr2.2015.05.013

Smith, R.A., J.R. Slack, T. Wyant, and K.J. Lanfear. 1982. *The Oil Spill Risk Analysis Model of the US Geological Survey.* US Geological Survey Open-File Report 80-687, 119 pp.

Socolofsky, S.A., and E.E. Adams. 2005. Role of slip velocity in the behavior of stratified multiphase plumes. *Journal of Hydraulic Engineering* 131(4):273–282, http://dx.doi.org/10.1061/(ASCE)0733-9429(2005)131:4(273).

Socolofsky, S.A., E.E. Adams, M.C. Boufadel, Z.M. Aman, O. Johansen, W.J. Konkel, D. Lindo, M.N. Madsen, E.W. North, C.B. Paris, and others. 2015. Intercomparison of oil spill prediction models for accidental blowout scenarios with and without subsea chemical dispersant injection. *Marine Pollution Bulletin* 96(1–2):110–126, http://dx.doi.org/10.1016/j.marpolbul.2015.05.039.

Socolofsky, S.A., E.E. Adams, and C.R. Sherwood. 2011. Formation dynamics of subsurface hydrocarbon intrusions following the Deepwater Horizon blowout. *Geophysical Research Letters* 38, L09602, http://dx.doi.org/10.1029/2011GL047174.

Speer, K., and J. Marshall. 1995. The growth of convective plumes at seafloor hot springs. *Journal of Marine Research* 53:1,025–1,057, http://dx.doi.org/10.1357/0022240953212972.

Spier, C., W.T. Stringfellow, T.C. Hazen, and M. Conrad. 2013. Distribution of hydrocarbons released during the 2010 MC252 oil spill in deep offshore waters. *Environmental Pollution* 173:224–230, http://dx.doi.org/10.1016/j.envpol.2012.10.019.

Walker, N.D., C.T. Pilley, V.V. Raghunathan, E.J. D'Sa, R.R. Leben, N.G. Hoffmann, P.J. Brickley, P.D. Coholan, N. Sharma, and H.C. Graber. 2011. Impacts of Loop Current frontal cyclonic eddies and wind forcing on the 2010 Gulf of Mexico oil spill. Pp. 103–116 in *Monitoring and Modeling the Deepwater Horizon Oil Spill: A Record-Breaking Enterprise.* Y. Liu, A. MacFadyen, Z.-G. Ji, and R.H. Weisberg, eds, American Geophysical Union, Washington, DC, http://dx.doi.org/10.1029/2011GM001120.

Wei, M.Z., C. Rowley, P. Martin, C.N. Barron, and G. Jacobs. 2014. The US Navy's RELO ensemble prediction system and its performance in the Gulf of Mexico. *Quarterly Journal of the Royal Meteorological Society* 140(681):1,129–1,149, http://dx.doi.org/10.1002/qj.2199.

Weisberg, R.H., L. Zheng, and Y. Liu. 2011. Tracking subsurface oil in the aftermath of the Deepwater Horizon well blowout. Pp. 205–215 in *Monitoring and Modeling the Deepwater Horizon Oil Spill: A Record-Breaking Enterprise.* Y. Liu, A. MacFadyen, Z.-G. Ji, and R.H. Weisberg, eds, American Geophysical Union, Washington, DC, http://dx.doi.org/10.1029/2011GM001131.

Yapa, P.D., M.R. Wimalaratne, A.L. Dissanayake, and J.A. DeGraff Jr. 2012. How does oil and gas behave when released in deepwater? *Journal of Hydro-Environment Research* 6(4):275–285, http://dx.doi.org/10.1016/j.jher.2012.05.002.

Yaremchuk, M., P. Spence, M. Wei, and G. Jacobs. 2013. Lagrangian predictability in the DWH region from HF radar observations and model output. *Deep Sea Research Part II* 129:394–400, http://dx.doi.org/10.1016/j.dsr2.2003.05.035.

Zheng, Y., M.A. Bourassa, and P. Hughes. 2013. Influences of sea surface temperature gradients and surface roughness changes on the motion of surface oil: A simple idealized study. *Journal of Applied Meteorology and Climatology*, http://dx.doi.org/10.1175/JAMC-D-12-0211.1.

Zhong, Y., A. Bracco, and T. Villareal. 2012. Pattern formation at the ocean surface: Sargassum distribution and the role of the eddy field. *Limnology and Oceanography, Fluids and Environments* 2:12–27, http://dx.doi.org/10.1215/21573689-1573372.

AUTHORS

Tamay M. Özgökmen (tozgokmen@rsmas.miami.edu) is Professor, Department of Ocean Sciences, Rosenstiel School of Marine and Atmospheric Science (RSMAS), University of Miami, Miami, FL, USA. **Eric P. Chassignet** is Director, Center for Ocean-Atmospheric Prediction Studies (COAPS), and Professor, Department of Earth, Ocean & Atmospheric Science (EOAS), Florida State University, Tallahassee, FL, USA. **Clint N. Dawson** is Professor and Head, Institute for Computational Engineering and Sciences, University of Texas Austin, Austin, TX, USA. **Dmitry Dukhovskoy** is Associate Research Scientist, COAPS, Florida State University, Tallahassee, FL, USA. **Gregg Jacobs** is Head, Ocean Dynamics and Prediction Branch, Naval Research Laboratory, Stennis Space Center, MS, USA. **James Ledwell** is Senior Scientist, Woods Hole Oceanographic Institution, Woods Hole, MA, USA. **Oscar Garcia-Pineda** is Director, WaterMapping LLC, Tallahassee, FL, USA. **Ian R. MacDonald** is Professor, EOAS, Florida State University, Tallahassee, FL, USA. **Steven L. Morey** is Research Scientist, COAPS, Florida State University, Tallahassee, FL, USA. **Maria Josefina Olascoaga** is Associate Professor, RSMAS, University of Miami, Miami, FL, USA. **Andrew C. Poje** is Professor, Department of Mathematics, City University of New York, New York, NY, USA. **Mark Reed** is Senior Research Scientist, SINTEF, Trondheim, Norway. **Jørgen Skancke** is Master of Science, SINTEF, Trondheim, Norway.